Hindawi Publishing Corporation
Journal of Nanomaterials
Volume 2012, Article ID 186138, 6 pages
doi:10.1155/2012/186138

Research Article

Effect of Low-Frequency Alternative-Current Magnetic Susceptibility in $Ni_{80}Fe_{20}$ Thin Films

Yuan-Tsung Chen, S. H. Lin, and Y. C. Lin

Department of Materials Science and Engineering, I-Shou University, Kaohsiung 840, Taiwan

Correspondence should be addressed to Yuan-Tsung Chen, ytchen@isu.edu.tw

Received 7 January 2012; Revised 6 February 2012; Accepted 6 February 2012

Academic Editor: Zhi Li Xiao

X-ray diffraction (XRD) results indicate that the NiFe thin films had a face-centered cubic (FCC) structure. Post-annealing treatment increased the crystallinity of NiFe films over those at room temperature (RT), suggesting that NiFe crystallization yields FCC (111) texturing. Post-annealing treatments increase crystallinity over that obtained at RT. This paper focuses on the maximum alternative-current magnetic susceptibility (χ_{ac}) value of NiFe thin films with resonance frequency (f_{res}) at low frequencies from 10 Hz to 25000 Hz. These results demonstrate that the χ_{ac} of NiFe thin films increased with post-annealing treatment and increasing thickness. The NiFe (111) texture suggests that the relationship between magneto-crystalline anisotropy and the maximum χ_{ac} value with optimal resonance frequency (f_{res}) increased spin sensitivity at optimal f_{res}. The results obtained under the three conditions revealed that the maximum χ_{ac} value and optimal f_{res} of a 1000 Å-thick NiFe thin film are 3.45 Hz and 500 Hz, respectively, following postannealing at $T_A = 250^\circ$C for 1 h. This suggests that a 1000 Å NiFe thin film post-annealed at $T_A = 250^\circ$C is suitable for gauge sensor and transformer applications at low frequencies.

1. Introduction

Researchers have recently focused on measuring alternative-current magnetic susceptibility (χ_{ac}) at low frequency. However, most studies on this topic have examined the magnetic susceptibility at high frequency. Interference of a magnetic field with signal is most difficult to deal with at low frequencies associated with alternating current (AC). When the applied magnetic field is an AC magnetic field and the AC frequency is not high, the magnetic dipole direction can vary with the field. As a result, the low-frequency alternative-current magnetic susceptibility (χ_{ac}) varies. NiFe film is an important soft magnetic material that has been extensively adopted in industry and the operation of read heads. The characteristics of such a film vary with Ni content [1]. A low coercive field is associated with approximately 80 at% Ni; high saturation magnetic induction is associated with around 50 at% Ni, and low susceptibility but high electrical resistivity is associated with about 35 at% Ni. Ni content also affects the stability of the resonance frequency and the initial susceptibility [2]. Generally, χ_{ac} is used at high frequency [3]. However, few studies have measured χ_{ac} at low frequency. The maximum χ_{ac} and optimal resonance frequency (f_{res}) are worthy of further study. The maximum χ_{ac} and optimal f_{res} demonstrate that the spin sensitivity is maximal at f_{res}. This can be exploited in low-frequency gauge sensor and transformer applications [4]. The benefits associated with low-frequency χ_{ac} are low power loss, low input power, and similarity to the magnetic properties of rocks, which is useful in environmental magnetism studies [5]. However, most studies in the field have extensively considered the applications of NiFe thin films at high frequency [6, 7]. Zawilski's theory provides a sounder theoretical basis for frequency of susceptibility application [7]. Some soft material experiments have been performed using $Ni_{80}Fe_{20}$ or CoFeB film because it has a high saturation magnetization (M_s), low coercivity (H_c), and a highly anisotropic field (H_k) for use in magnetoresistance random access memory (MRAM) applications [8–11]. Some studies have discussed the benefits of alternative magnetic susceptibility measurement approaches, such as using a wide range of frequencies from 10 Hz to 25000 Hz in investigations of environmental

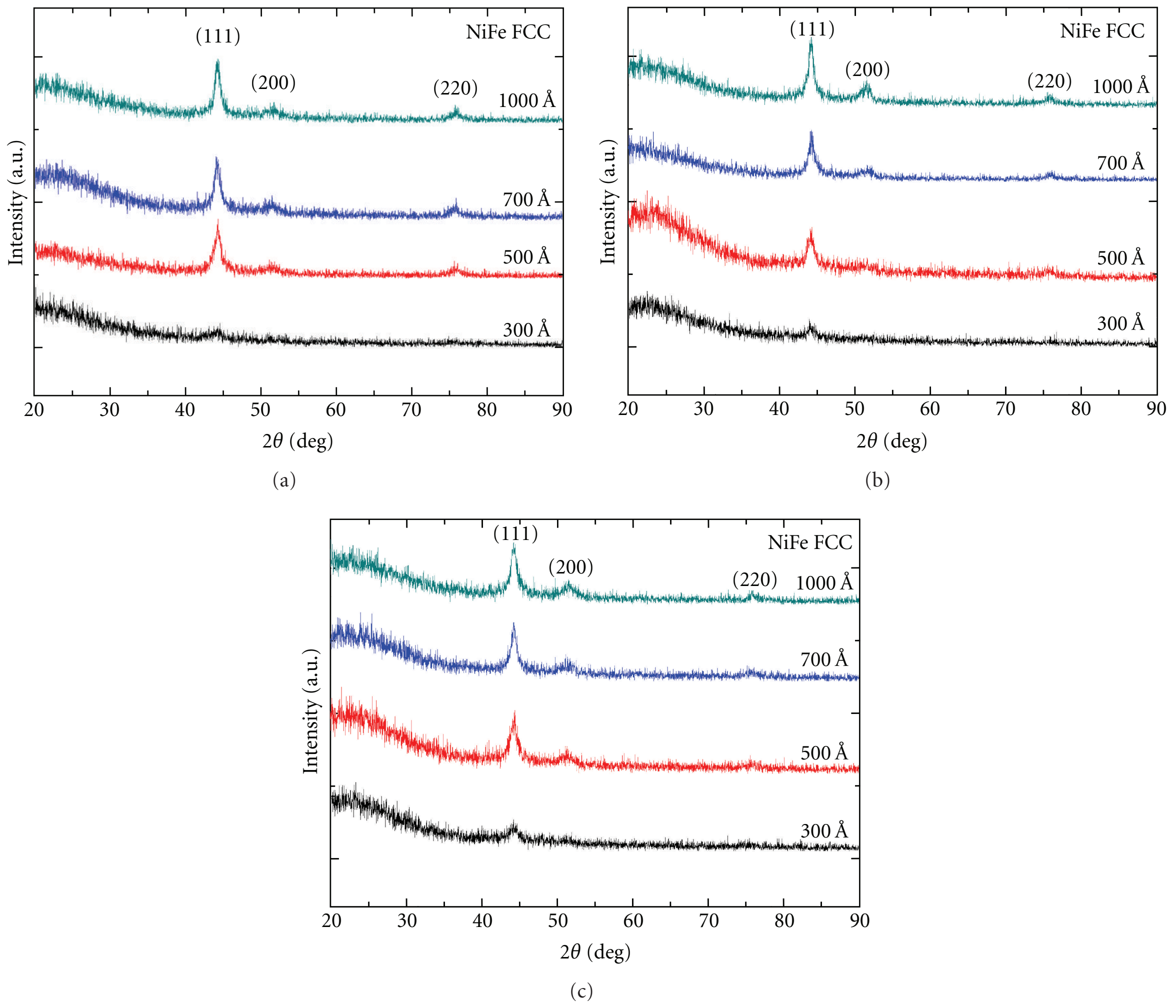

Figure 1: X-ray diffraction patterns of NiFe films with thicknesses from 300 Å to 1000 Å under three preparation conditions: (a) deposited at RT only, (b) postannealed at $T_A = 150^\circ$C for 1 h, and (c) postannealed at $T_A = 250^\circ$C for 1 h.

magnetism even if to estimate the distribution of grain sizes of superparamagnetic particles and to determine the critical temperature (T_c) of ferromagnetic materials [12].

This work uses $Ni_{80}Fe_{20}$ films of various thicknesses to measure alternative-current magnetic susceptibility (χ_{ac}) and resonance frequency (f_{res}) at various temperatures and various frequencies of the current. X-ray diffraction (XRD) reveals that the NiFe thin films have a face-centered cubic (FCC) (111) textured structure and postannealed NiFe films are more crystalline than those formed at RT. The magneto-crystalline anisotropy of the (111) texture can be reasonably concluded to indicate that the maximum χ_{ac} value is associated with the optimal resonance frequency (f_{res}).

2. Experimental Details

NiFe thin films with a thickness (t_f) of between 300 Å and 1000 Å were deposited on a glass substrate by DC magnetron sputtering under three conditions: (a) T_s sustained at RT; (b) T_s = RT, followed by post-annealing at $T_A = 150^\circ$C for 1 h; (c) T_s = RT, followed by post-annealing at $T_A = 250^\circ$C for 1 h. The typical base chamber pressure was less than 1×10^{-7} Torr, and the Ar-working chamber pressure was 5×10^{-3} Torr. The target composition of the NiFe alloy was 80 at % Ni and 20 at % Fe.

The structure of the NiFe thin film was elucidated by X-ray diffraction (XRD), employing a $CuK_{\alpha 1}$ line (Philips X′pert). The in-plane low-frequency alternative-current magnetic susceptibility (χ_{ac}) was examined using an χ_{ac} analyzer (XacQuan, MagQu) to remove the demagnetization factor. The driving frequency ranged from 10 Hz to 25 000 Hz. The same shape and size of each sample were measured.

3. Results and Discussion

Figure 1 displays the X-ray diffraction patterns of NiFe films under three conditions. Figures 1(a) to 1(c) present the X-ray results for the films formed at RT, with postannealing at $T_A = 150^\circ$C and at $T_A = 250^\circ$C, respectively. They include significant crystalline peaks in the 2θ range of 20°–90°, including peaks associated with a highly crystalline (111)

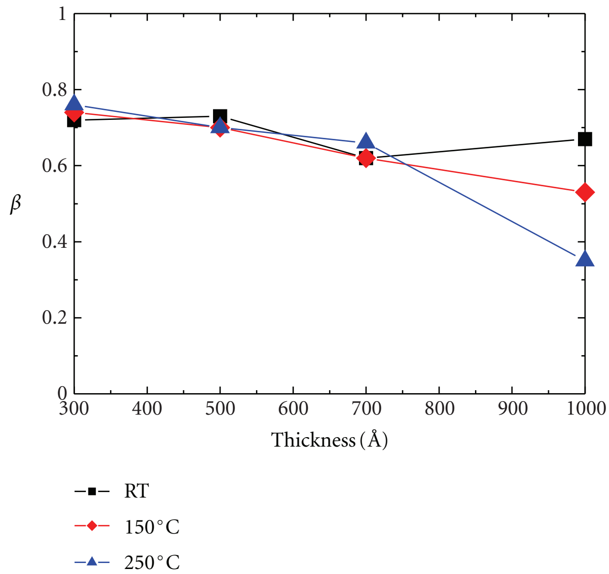

Figure 2: FWHM (β) of NiFe (111) peak as a function of thickness of NiFe thin films prepared under three conditions.

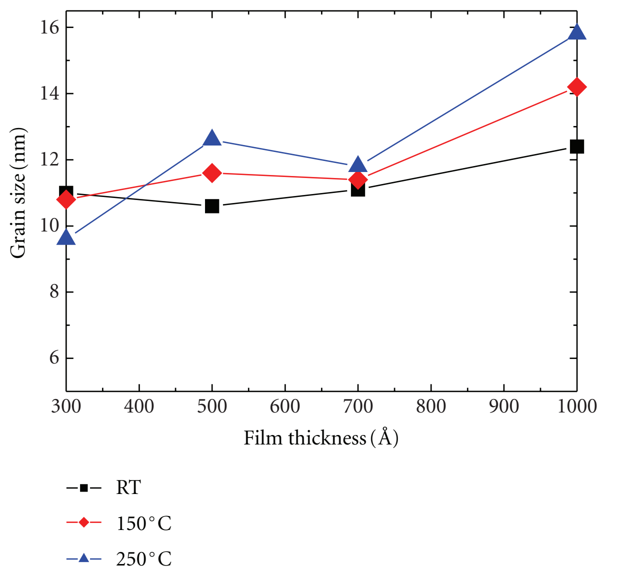

Figure 3: Grain size as a function of thickness of NiFe thin films prepared under three conditions.

diffraction peak and two weak (200), (220) peaks. XRD results indicate that the resulting NiFe thin films have a face-centered cubic (FCC) structure. The apparent (111) peak of the NiFe thin films measuring 500 Å, 700 Å, or 1000 Å thick revealed a greater diffracted intensity than the (200) and (220) peaks. The intensity of the NiFe (111) peak is three times stronger than the (200) and (220) peaks. This implies the relationship between FCC (111) texturing and NiFe crystallization. Corresponding to other NiFe thickness, the XRD intensity of the films with a thickness of 300 Å formed under three conditions is very weak, but the peaks still exist. This suggests that the film growth model is imperfect. The diffraction peaks of the NiFe thin films become more crystalline as the thickness increases. The crystallization achieved by annealing treatment exceeds that achieved at RT because the thermal energy can drive grain growth.

Figure 2 plots the corresponding full width at half maximum (FWHM, β) of the NiFe (111) peak at three different thicknesses. The XRD diffraction result indicates that the intensity of the NiFe (111) peak is much larger than other (200) and (220) peaks. Figure 3 shows the half maximum (FWHM, β) of the NiFe (111) peak to estimate the grain size distribution under three conditions and different NiFe thicknesses. Figure 2 shows that a thinner NiFe film yields a larger FWHM, and the FWHM for films formed at RT is larger than that of films that have undergone post-annealing.

Scherrer's formula enables estimating the mean crystallite grain size (D) from the measured width of the diffraction peak under crystalline quality of three conditions, as Figure 3 shows. Scherrer's formula is [13]

$$D = \frac{k\lambda}{\beta \cos\theta}, \tag{1}$$

where k (0.89) is Scherrer's constant, λ is the X-ray wavelength of the CuK$_{\alpha 1}$ line, β is the relative value of the full width at half maximum (FWHM) of the (111) peak, and θ is the half angle of the diffraction peak. The formula states that D is proportional to $1/\beta$, and, thus, a larger β corresponds to smaller grains. For example, Scherrer's formula yields grain sizes of 124 Å, 142 Å, and 158 Å, respectively, for 1000 Å-thick NiFe thin films (a) with a substrate temperature (T_s) maintained at RT, (b) after post-annealing at $T_A = 150°C$ for 1 h, and (c) after post-annealing at heat annealing $T_A = 250°C$ for 1 h. This distribution of grain sizes is consistent with XRD results.

Figures 4(a) to 4(c) plot the alternative-current magnetic susceptibility (χ_{ac}) as a function of thickness at low frequency for NiFe films under the three preparation conditions. Apparently, no 300 Å-thick NiFe thin film, formed under any condition, yields an apparent χ_{ac} signal at 10 Hz to 25 000 Hz. This result is consistent with the weak XRD diffraction crystalline results. Figure 4(a) shows that, at room temperature (RT), χ_{ac} increases with thickness at a frequency range of 10 Hz to 30 Hz, but decreases with increasing thickness at a frequency range of 30 Hz to 50 Hz. Additionally, χ_{ac} of 1000 Å-thick NiFe film reaches the corresponding maximum χ_{ac} value at 50 Hz to 100 Hz, and χ_{ac} again decreases with increasing thickness between 100 Hz and 25 000 Hz. Figure 4(a) showed that the maximum χ_{ac} value and optimal resonance frequency (f_{res}) for a 1000 Å-thick NiFe thin film following RT treatment are 1.36 Hz and 100 Hz, respectively. Figures 4(b) and 4(c) show the same trend of χ_{ac} of the NiFe films as a function of low frequency. The χ_{ac} value first increases from 10 Hz to 30 Hz, and then falls from 30 Hz to 50 Hz under conditions (b) and (c). The χ_{ac} of post-annealed films reaches its value in the 50 Hz to 500 Hz frequency range before falling as the frequency rises from 500 Hz to 25 000 Hz. Figure 4(b) shows that the maximum χ_{ac} value and optimal resonance frequency (f_{res})

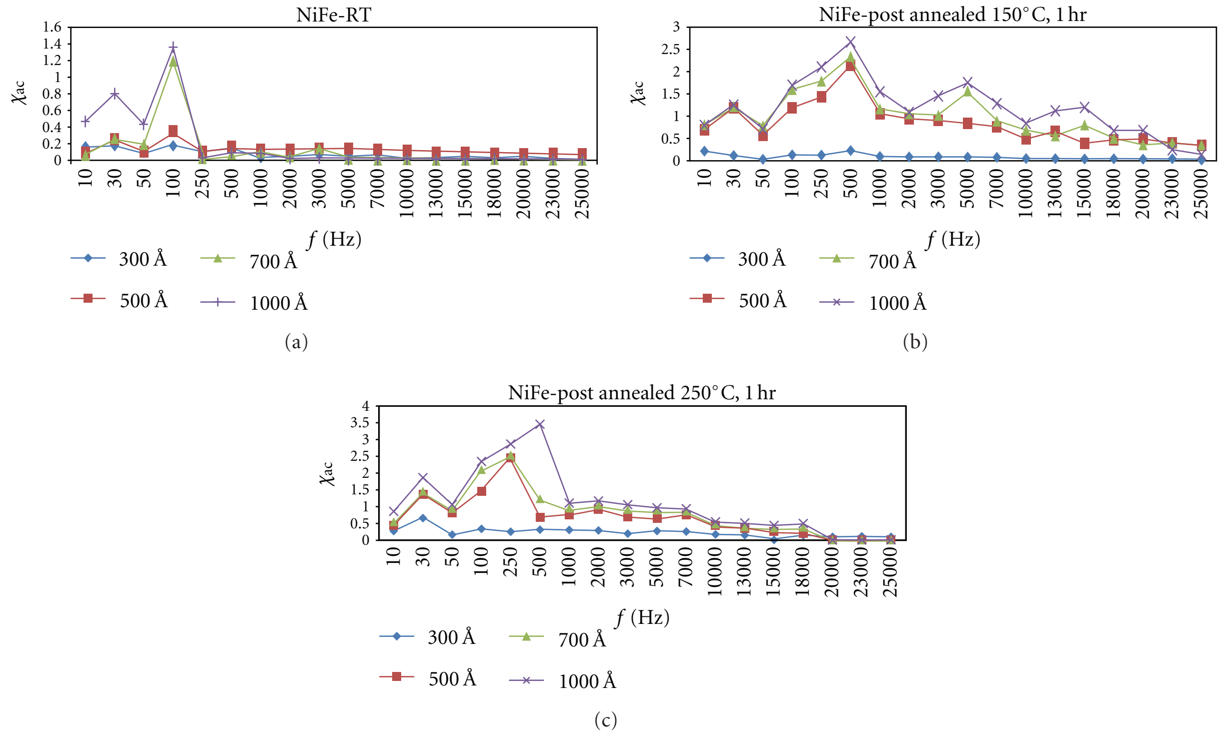

Figure 4: Alternative-current magnetic susceptibility (χ_{ac}) as a function of low frequency for NiFe films under three preparation conditions: (a) deposited at RT only, (b) postannealed at $T_A = 150°C$ for 1 h, and (c) postannealed at $T_A = 250°C$ for 1 h.

of a 1000 Å-thick NiFe thin film that has undergone post-annealing at $T_A = 150°C$ for 1 h are 2.66 Hz and 500 Hz, respectively. Figure 4(c) shows that the corresponding values of a film that has been post-annealed at $T_A = 250°C$ for 1 h are 3.45 Hz and 500 Hz, respectively. Apparently, the maximum χ_{ac} value achieved following post-annealing at $T_A = 250°C$ is 2.54 times that of a film prepared at RT. The results in Figure 4 show that post-annealing treatment increases χ_{ac} because the magneto-crystalline anisotropy of (111) texture effect induces the maximum χ_{ac} value with optimal resonance frequency (f_{res}) [14]. The optimal resonance frequency (f_{res}) is that at which the spin sensitivity is highest, suggesting that a 1000 Å-thick NiFe thin film that has been post-annealed at $T_A = 250°C$ is suitable for use in a gauge sensor and transformer applications at low frequency. However, a 300 Å-thick NiFe thin film under any one of the three conditions is not suitable because it yields no apparent χ_{ac} signal. The alternative-current magnetic susceptibility is generally correlated with film thickness and post-annealing temperature.

Figure 5 shows the results obtained at three temperatures for films of various thicknesses, including the maximum alternative-current magnetic susceptibility under three preparation conditions. The figure indicates that the maximum χ_{ac} increases with NiFe thickness. The 1000 Å-thick NiFe thin film yielded the highest χ_{ac} signal and corresponding optimal f_{res} under all conditions. Furthermore, the maximum χ_{ac} values of the films post-annealed films at $T_A = 150°C$ for 1 h and $T_A = 250°C$ for 1 h were significantly higher than the film prepared at RT. The 1000 Å-thick NiFe

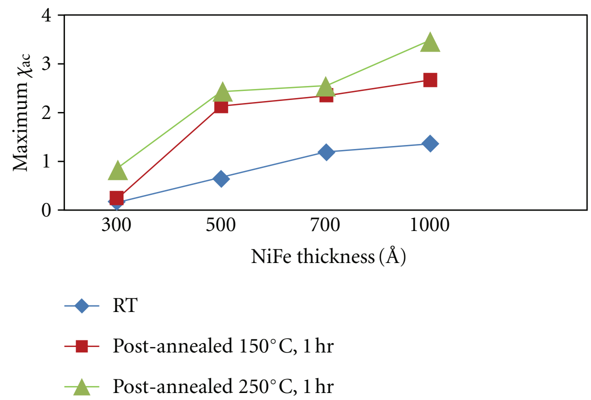

Figure 5: Maximum χ_{ac} at three temperatures and film thicknesses.

thin film that was post-annealed at $T_A = 250°C$ for 1 h had the highest χ_{ac}. These results show that the low-frequency alternative-current magnetic susceptibility is closely related to temperature, thickness, and resonant frequency.

Figure 6 plots the optimal frequency (f_{res}) associated with the maximum χ_{ac} value as a function of NiFe thickness under three preparation conditions. This figure demonstrates that the optimal f_{res} increases with thickness at RT. Additionally, the optimal resonant frequency post-annealing treatment at $T_A = 150°C$ for 1 h increases to saturation at 500 Hz. The optimal post-annealing treatment initially increases from 30 Hz to 250 Hz, whereas post-annealing at $T_A = 250°C$ for 1 h causes saturation at 500 Hz. Figures 5 and

Table 1: Maximum alternative-current magnetic susceptibility and optimal frequency at various thicknesses and temperatures.

NiFe thickness	Room temperature of maximum χ_{ac}	Post-annealed 150°C-1 hr of maximum χ_{ac}	Post-annealed 250°C-1 hr of maximum χ_{ac}	Highest χ_{ac} corresponding optimal resonance frequency f_{res} (Hz)
300 Å	0.172299	0.212215	0.85171	30 Hz
500 Å	0.661307	2.148086	2.456315	250 Hz
700 Å	1.194991	2.344501	2.541269	250 Hz
1000 Å	1.360231	2.668716	3.456921	500 Hz

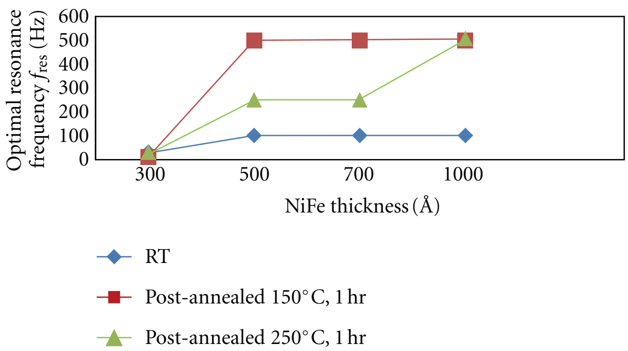

Figure 6: Maximum χ_{ac} at corresponding resonance frequency f_{res}.

6 suggest that the maximum χ_{ac} value and optimal resonance frequency (f_{res}) of a 1000 Å-thick NiFe thin film that has been post-annealed at $T_A = 250°C$ for 1 h are 3.45 Hz and 500 Hz, respectively.

Table 1 shows this relationship. Clearly, increasing post-annealing temperature, thickness, and resonance frequency positively affect χ_{ac} value. This result supports previous research showing that annealing has a positive effect on the magnetic property of the electroplated NiFe film [15]. The effect of thickness on the alternative-current magnetic susceptibility of $Ni_{80}Fe_{20}$ films is related to the degree of crystallinity [16]. The degree of crystallinity in thin film strongly affected the magnetic anisotropic field, magnetic coercivity, and relative susceptibility, which in turn affected magnetic properties [17, 18].

4. Conclusions

In conclusion, post-annealing treatment positively affects the alternative-current magnetic susceptibility, χ_{ac}, because the NiFe (111) texture induces the magneto crystalline anisotropy. This in turn results in a high χ_{ac} value and high spin sensitivity. The maximum χ_{ac} value and optimal resonance frequency (f_{res}) of a 1000 Å-thick NiFe thin film that was post-annealed at $T_A = 250°C$ for 1 h are 3.45 Hz and 500 Hz, respectively, under preparation conditions, suggesting that a 1000 Å-thick NiFe thin film post-annealed $T_A = 250°C$ is suitable for use in gauge sensors and transformer applications at low frequency. Increasing the thickness of an NiFe film increases its crystallinity, strongly affecting the magnetic anisotropy field, magnetic coercivity, and relative magnetic susceptibility.

Acknowledgment

This paper was supported by the National Science Council, under Grant no. NSC100-2112-M214-001-MY3.

References

[1] H. Fujiwara, K. Nishioka, C. Hou, M. R. Parker, S. Gangopadhyay, and R. Metzger, "Temperature dependence of the pinning field and coercivity of NiFe layers coupled with an antiferromagnetic FeMn layer," *Journal of Applied Physics*, vol. 79, no. 8, pp. 6286–6288, 1996.

[2] Y. Liu, J. Zhang, L. Yu, G. Jia, C. Jing, and S. Cao, "Magnetic and frequency properties for nanocrystalline Fe-Ni alloys prepared by high-energy milling method," *Journal of Magnetism and Magnetic Materials*, vol. 285, no. 1-2, pp. 138–144, 2005.

[3] K. H. Kim, J. H. Jeong, J. Kim, S. H. Han, and H. J. Kim, "High moment and high frequency permeability Fe-B-N nanocrystalline soft magnetic films," *Journal of Magnetism and Magnetic Materials*, vol. 239, no. 1–3, pp. 487–489, 2002.

[4] Y. T. Chen and Z. G. Chang, "Low-frequency alternative-current magnetic susceptibility of amorphous and nanocrystalline $Co_{60}Fe_{20}B_{20}$ films," *Journal of Magnetism and Magnetic Materials*, vol. 324, no. 14, pp. 2224–2226, 2012.

[5] K. Kodama, "A new system for measuring alternating current magnetic susceptibility of natural materials over a wide range of frequencies," *Geochemistry, Geophysics, Geosystems*, vol. 11, no. 11, article Q11002, 7 pages, 2010.

[6] T. O'Donnell, N. Wang, S. Kulkarni et al., "Electrodeposited anisotropic NiFe 45/55 thin films for high-frequency micro-inductor applications," *Journal of Magnetism and Magnetic Materials*, vol. 322, no. 9–12, pp. 1690–1693, 2010.

[7] B. M. Zawilski, J. Marcus, and P. Plaindoux, "A simple and accurate relative alternative magnetic susceptibility measurement technique," *Journal of Magnetism and Magnetic Materials*, vol. 322, no. 18, pp. 2786–2788, 2010.

[8] S. Ito, T. Okamoto, S. H. Kong, and S. Nakagawa, "Fe-Co-B/[Ni-Fe/Si] soft magnetic underlayer with high anisotropy field along cross-track direction on disk substrate," *Journal of Magnetism and Magnetic Materials*, vol. 287, pp. 281–286, 2005.

[9] P. Holland, M. Kempton, D. Ragan et al., "The magnetic hysteresis of NiFe-31% thin films under isotropic in-plane stress," *Journal of Magnetism and Magnetic Materials*, vol. 250, pp. L1–L5, 2002.

[10] S. K. Wang, Y. T. Chen, and S. R. Jian, "Determining contact angle and surface energy of $Co_{60}Fe_{20}B_{20}$ thin films by magnetron sputterin," *Journal of Nanomaterials*, vol. 2011, Article ID 291935, 4 pages, 2011.

[11] Y. T. Chen and S. M. Xie, "Magnetic and electric properties of amorphous $Co_{40}Fe_{40}B_{20}$ thin films," *Journal of Nanomaterials*, vol. 2012, Article ID 486284, 5 pages, 2012.

[12] C. Opagiste, M. Couach, A. Khoder et al., "Reversibility of the mixed state of the 107K $Tl_2Ba_2CaCu_2O_8$ superconductor investigated by different susceptibility measurements," *Physica B*, vol. 194–196, no. 2, pp. 1809–1810, 1994.

[13] B. D. Cullity, *Elements of X-ray Diffraction*, Addison-Wesley, Reading, Mass, USA, 2nd edition, 1978.

[14] Y. T. Chen and J. W. Wu, "Effect of tunneling barrier as spacer on exchange coupling of CoFeB/AlO_x/Co trilayer structures," *Journal of Alloys and Compounds*, vol. 509, no. 37, pp. 9246–9248, 2011.

[15] T. Budde and H. H. Gatzen, "Magnetic properties of an SmCo/NiFe system for magnetic microactuators," *Journal of Magnetism and Magnetic Materials*, vol. 272–276, no. 3, pp. 2027–2028, 2004.

[16] Y. M. Kim, D. Choi, K. H. Kim, K. H. Kim, S.H. Han, and H.J. Kim, "Thickness effects on the high-frequency characteristics of as-deposited Co-Ni-Fe and Co-Ni-Fe-N soft magnetic thin films," *Journal of Magnetism and Magnetic Materials*, vol. 239, no. 1–3, pp. 498–501, 2002.

[17] T. Suetsuna, S. Suenaga, S. Sakurada, K. Harada, M. Tomimatsu, and T. Takahashi, "Effects of crystalline grain size and packing ratio of self-forming core/shell nanoparticles on magnetic properties at up to GHz bands," *Journal of Magnetism and Magnetic Materials*, vol. 323, no. 13, pp. 1793–1798, 2011.

[18] W. Tang, Z. Q. Jin, J. R. Zhang, G. Gu, J. M. Li, and Y. W. Du, "Effect of composition on crystalline texture and magnetic properties of $Nd_2Fe_{14}B$ thin films," *Journal of Magnetism and Magnetic Materials*, vol. 185, no. 2, pp. 241–245, 1998.

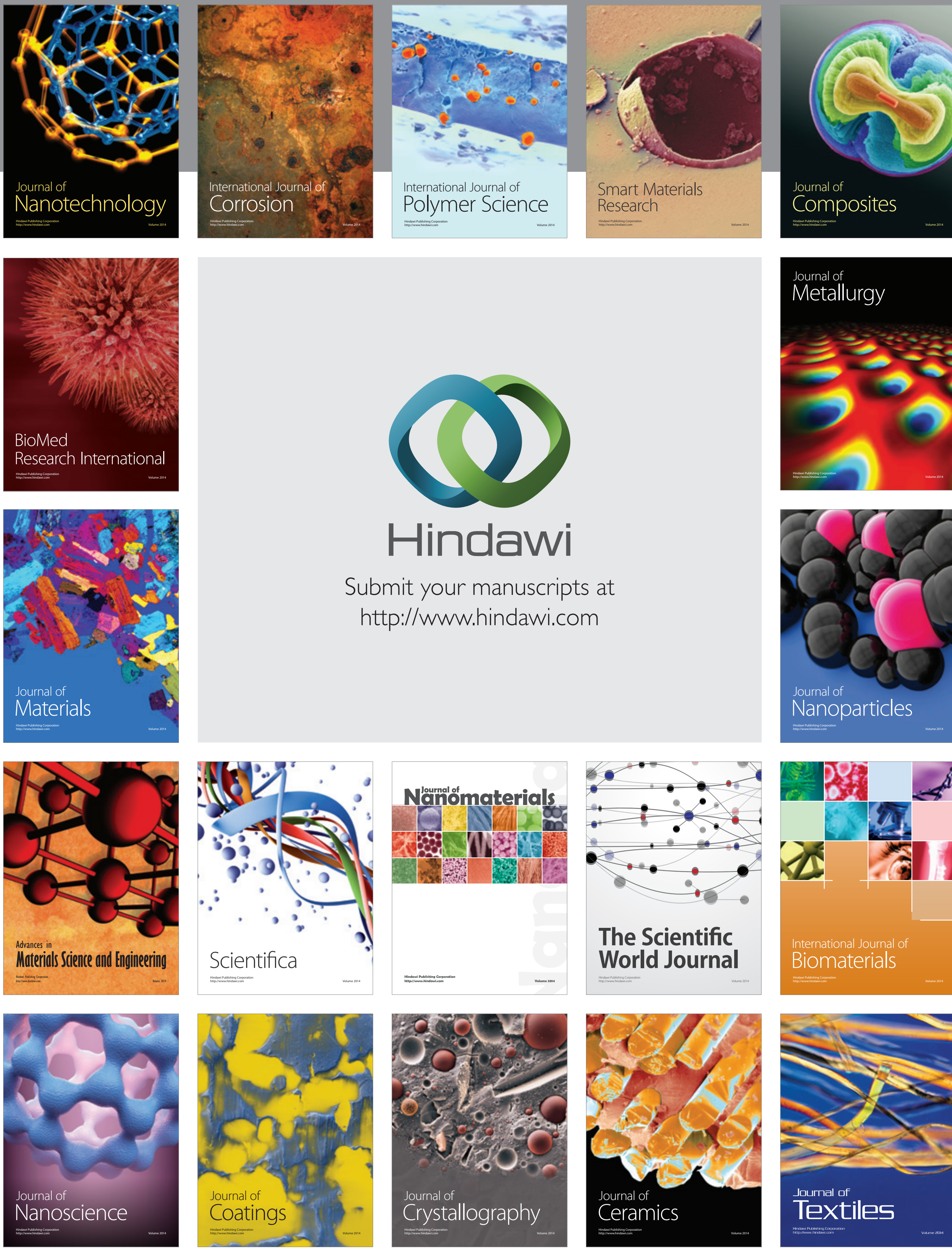
Journal of Nanotechnology
International Journal of Corrosion
International Journal of Polymer Science
Smart Materials Research
Journal of Composites
BioMed Research International
Journal of Metallurgy
Hindawi
Submit your manuscripts at
http://www.hindawi.com
Journal of Materials
Journal of Nanoparticles
Advances in Materials Science and Engineering
Scientifica
Journal of Nanomaterials
The Scientific World Journal
International Journal of Biomaterials
Journal of Nanoscience
Journal of Coatings
Journal of Crystallography
Journal of Ceramics
Journal of Textiles